DRUG FORMULATIONS AND CLINICAL METHODS

Design of a Sensitive and Selective Electrochemical Aptasensor for the Determination of the Complementary cDNA of miRNA-145 Based on the Intercalation and Electrochemical Reduction of Doxorubicin

MARYAM MOHAMADI
Pistachio Safety Research Center, Rafsanjan University of Medical Sciences, Rafsanjan, Iran
ALI MOSTAFAVI
Shahid Bahonar University of Kerman, Faculty of Science, Department of Chemistry, Kerman, Iran
MASOUD TORKZADEH-MAHANI
Graduate University of Advanced Technology, Institute of Science and High Technology and Environmental Sciences, Department of Biotechnology, Kerman, Iran

The aim of this research was the determination of a microRNA (miRNA) using a DNA electrochemical aptasensor. In this biosensor, the complementary complementary DNA (cDNA) of miRNA-145 (a sense RNA transcript) was the target strand and the cDNA of miRNA-145 was the probe strand. Both cDNAs can be the product of the reverse transcriptase-polymerase chain reaction of miRNA. The proposed aptasensor's function was based on the hybridization of target strands with probes immobilized on the surface of a working electrode and the subsequent intercalation of doxorubicin (DOX) molecules functioning as the electroactive indicators of any double strands that formed. Electrochemical transduction was performed by measuring the cathodic current resulting from the electrochemical reduction of the intercalated molecules at the electrode surface. In the experiment, because many DOX molecules accumulated on each target strand on the electrode surface, amplification was inherently easy, without a need for enzymatic or complicated amplification strategies. The proposed aptasensor also had the excellent ability to regenerate as a result of the melting of the DNA duplex. Moreover, the use of DNA probe strands obviated the challenges of working with an RNA probe, such as sensitivity to RNase enzyme. In addition to the linear relationship between the electrochemical signal and the concentration of the target strands that ranged from 2.0 to 80.0 nM with an LOD of 0.27 nM, the proposed biosensor was clearly capable of distinguishing between complementary (target strand) and noncomplementary sequences. The presented biosensor was successfully applied for the quantification of DNA strands corresponding to miRNA-145 in human serum samples.

Received September 16, 2016. Accepted by SW March 13, 2017.
Corresponding author's e-mail: m.mohamadi794@gmail.com
DOI: 10.5740/jaoacint.16-0302

Aptamers are single-stranded oligonucleotides that are 15–40 bases long and generated in vitro by a process known as the systematic evolution of ligands by exponential enrichment (1). Because aptamers can specifically bind to certain targets with extremely high specificity, they are considered chemical antibodies. Thus, aptamers, especially DNA aptamers, represent a new generation of biomolecules that are mostly used as a recognition element in biosensors (2). In addition to molecular recognition, signal transduction is another essential characteristic of biosensors, which determines changes in the recognition layer caused by a target species (3). Among the different transducers, those applying electrochemical techniques are viewed as particularly attractive alternatives for bioanalysis because of their readily available signal transduction, high sensitivity and accuracy, low LOD, low cost, and ease of automatization (4–8).

MicroRNAs (miRNAs) are short regulatory RNAs containing 18–24 nucleotides that settle into an RNA-induced silencing complex and arrest translation. miRNAs are involved in numerous biological processes, including organ development, cellular proliferation, tissue differentiation, and apoptosis by controlling translation via inducing the degradation of target messenger RNAs (9, 10). It has been found that alterations in miRNA are involved in the initiation and progression of human cancers. Recent evidence indicates that miRNAs can function as tumor suppressors and oncogenes and have been, therefore, referred to as oncomirs (11). miRNA-145, with a sequence of 5′-GUCCAGUUUUCCCAGGAAUCCCU-3′ in its mature form, is a well-known tumor-suppressing miRNA whose expression level is decreased in numerous human cancers, such as breast (12), colon (13), lung (14), liver (15), bladder (16), pituitary (17), ovarian (18), and prostate (19). Thus, down-regulation of miRNA-145 is an early event in many cancers, suggesting its expression could be useful for the monitoring and early detection of cancer.

Due to the short length of mature miRNAs and their occurrence in low concentrations as consequence of decreased miRNA expression during most active cancers, using conventional methods for the detection and quantification of miRNAs is discouraged because they are time-consuming and problematic. Therefore, there is a crucial need to develop accurate, rapid, and sensitive methods for the detection of miRNAs (20).

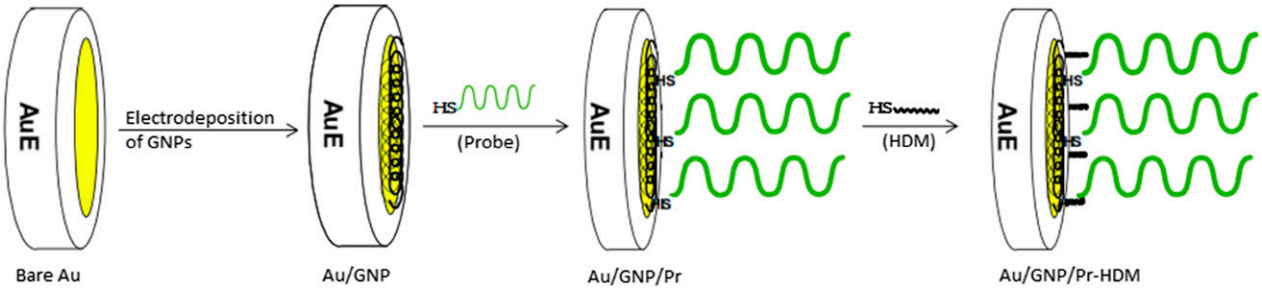

Figure 1. Schematic illustration of the stepwise fabrication of the biosensor.

Electrochemical biosensors are one of the most attractive techniques for this purpose. A typical electrochemical biosensor is made of a solid electrode on which short, single-stranded probes complementary to the strand of interest are immobilized and function as one or more electroactive hybridization indicators. Hybridization between the probe and the complementary sequence (the target) influences the performance of the electrochemical biosensor (21). Several approaches have been reported for signal amplification, such as nanomaterials (22), enzymes (23), electroactive complexes (24), and the electrocatalytic oxidation of guanine (25).

RNA, however, is less stable than DNA and also requires special working conditions. For example, RNA is highly sensitive to RNase: RNase is stable up to 300 °C, whereas DNase can be degraded by autoclaving (26). Consequently, reverse transcriptase-polymerase chain reaction (RT-PCR) can be used to convert the RNA of interest into its complementary DNA (cDNA) using reverse transcriptase and deoxynucleotides. The newly synthesized cDNA is then used as a template for the exponential amplification and production of DNA strands with a sequence equivalent to the sequence of the initial RNA (complementary cDNA) using polymerase in a PCR protocol (27).

Therefore, we used probe and target strands in the present work that are DNA rather than RNA. Herein, we propose a simple, sensitive, low-cost, and specific aptasensor for the determination of miRNA-145 DNA strands via cDNA strands immobilized on the surface of a working electrode. In fact, we used the sequence of the products of RT-PCR of miRNA-145 (cDNA as the probe and complementary cDNA as the target) to design the electrochemical aptasensor. In this approach there is no need for labeling, electrocatalysis, or enzymatic amplification, all of which are complicated and expensive processes. Instead, we used an electroactive intercalator, doxorubicin (DOX), for the electrochemical transduction of hybridization.

Experimental

Apparatus

All voltammetric experiments were performed with a 757 VA Computrance electrochemical system from Metrohm (Herisau, Switzerland) interfaced with a personal computer for data acquisition and potential control. A three-electrode assembly was used: a glass cell containing a silver (Ag)/AgCl electrode as the reference electrode, a platinum wire as the counter electrode, and a gold (Au) electrode, with an area of 0.0314 cm^2, as the working electrode. A Metrohm 827 pH meter equipped with a combined glass reference electrode was used to measure pH.

Chemicals and Reagents

A standard solution of 1000 mg L^{-1} Au(III) was obtained from Merck (Darmstadt, Germany). 1-Hexadecyl mercaptane was purchased from Aldrich (Steinheim, Germany). A standard solution of 4.3 mM DOX was obtained from Pharma EBEWE Ges (Unterach, Austria). All other chemicals were of analytical grade. Oligodeoxynucleotide samples were obtained from Alpha DNA (Montreal, Canada) and had the following sequences:

(**a**) *Probe strand.*—5′-SH(CH2)6-AGGGATTCCTGGGAA AACTGGAC-3′.

(**b**) *Target strand.*—3′-GTCCAGTTTTCCCAGGAATCCCT-5′.

(**c**) *Noncomplementary strand A.*—3′-C CGC TGC TCA GGT CCC CCT GGG GAT-5′.

(**d**) *Noncomplementary strand B.*—3′-AGC CAG CCC GCA CAC AAA CAC AGG-5′.

The buffer solutions used in this study were as follows:

(**a**) *Probe immobilization buffer.*—10× Tris-NaCl-EDTA (TNE), pH 7.0.

(**b**) *Hybridization buffer.*—1× saline sodium citrate (SSC), pH 7.0.

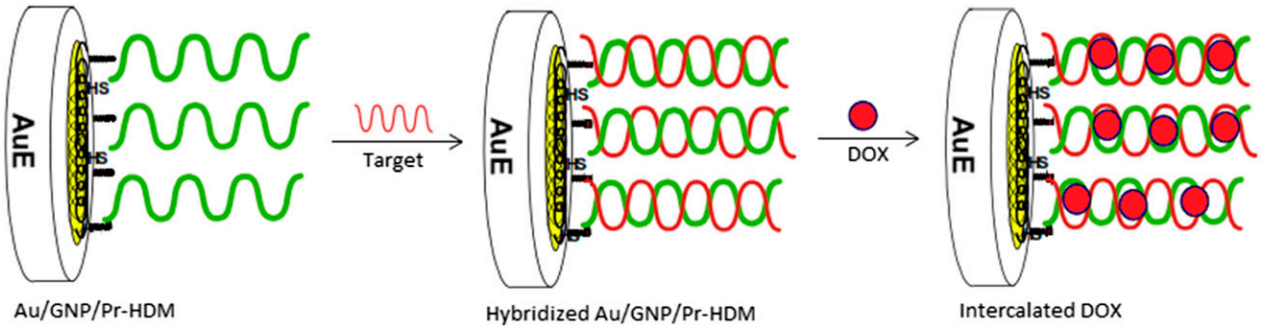

Figure 2. Schematic illustration showing the use of the biosensor for the detection of the target strand.

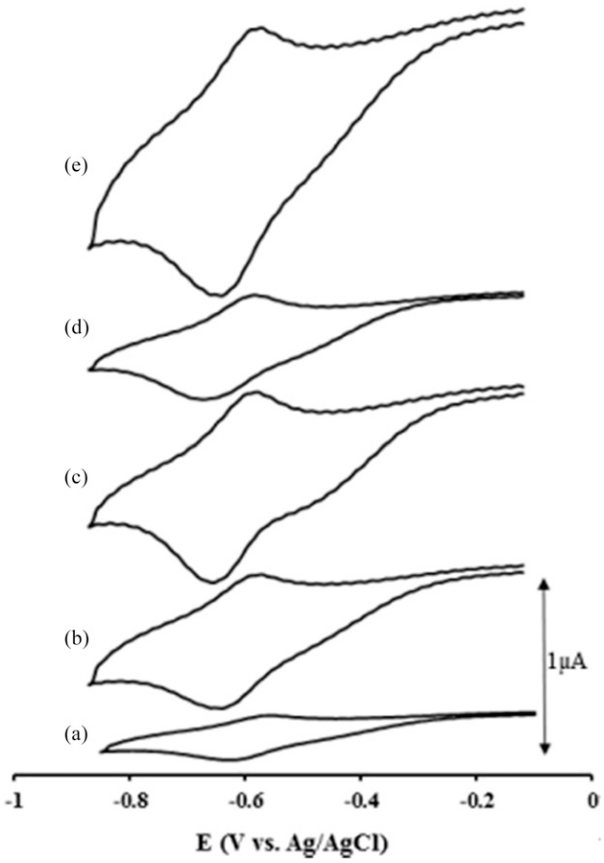

Figure 3. Cyclic voltammograms of DOX accumulated on the surface of the (a) bare Au electrode, (b) Au/GNP, (c) Au/GNP/Pr, (d) Au/GNP/Pr-HDM, and (e) Au/GNP/Pr-HDM after hybridization with 30 nM of the target strand in SSC buffer for 40 min. Conditions: 10 µM DOX in phosphate buffer, accumulation time of 15 min, supporting electrolyte phosphate buffer, and scan rate of 500 mV s^{-1}.

(**c**) *Hexadecanethiol (HDM) immobilization buffer*.—Tris–HCl 0.01 M, pH 7.0.

(**d**) *DOX intercalation buffer*.—Phosphate 0.05 M, pH 7.0.

(**e**) *Electrochemical determination buffer*.—Phosphate 0.05 M, pH 7.0.

Preparation of the Biosensor

The step-by-step preparation of Au/gold nanoparticle (GNP)/praseodymium (Pr)-HDM is schematically depicted in Figure 1 and described below.

Electrochemical Deposition of GNPs

The Au electrode was carefully polished to a mirror-like surface with 0.05 mm alumina slurries, followed by its consecutive ultrasonication in distilled water, acetone, and distilled water for 1 min for each step. Subsequently, the electrode was electrochemically pretreated in 0.5 M H_2SO_4 aqueous solution using sweeping in the potential range of 0 to + 1.5 V at a potential scan rate of 100 mV s^{-1} until a cyclic voltammogram characteristic of a clean Au electrode was obtained, after which the Au electrode was thoroughly washed with distilled water. For the deposition of GNPs on the surface of the cleaned Au electrode, the previously reported

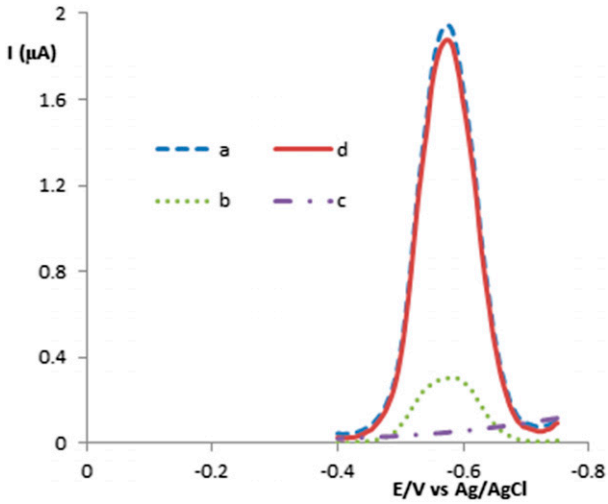

Figure 4. Differential pulse-stripping voltammograms of DOX at the surface of Au/GNP/Pr-HDM (a) after hybridization with 50 nM of the target strand, (b) after immersing the electrode (a) in a water bath, (c) after immersing electrode (b) in 0.1 M phosphate-buffered saline, and (d) after hybridization of the refreshed electrode (c) with 50 nM of the target strand.

electrochemical procedure (20) was applied. Briefly, the electrode was immersed into 0.1 M KNO_3 solution containing 3 mM $HAuCl_4$. A potential of –0.2 V was applied to the electrode for 300 s while the solution was stirred. Finally, the electrode was washed with distilled water and dried at room temperature. The modified electrode obtained was designated "Au/GNP."

Immobilization of Probe Strands

Au/GNP was immersed in TNE buffer containing 1.2 µM of the probe strand and incubated for 12 h at room temperature. During this time, the HS-modified probe strands self-assembled on the surface of Au/GNP. The probe-modified electrode was immersed into blank TNE buffer for 1 h under constant stirring to remove any nonadsorbed strands. The modified electrode obtained was thoroughly washed with TNE buffer and designated "Au/GNP/Pr."

Immobilization of HDM

To eliminate probe strands that had been nonspecifically adsorbed and retain good strand orientation and recognition ability, HDM molecules were immobilized between the probe

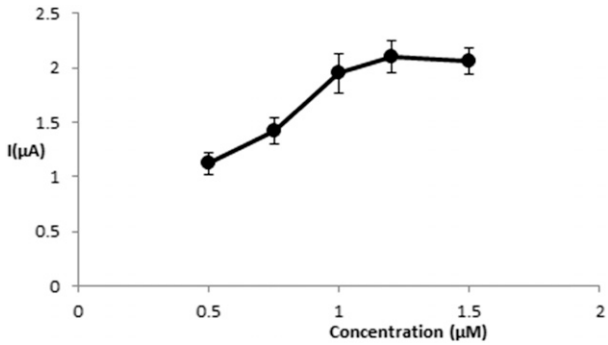

Figure 5. Effect of probe concentration on the peak current of DOX.

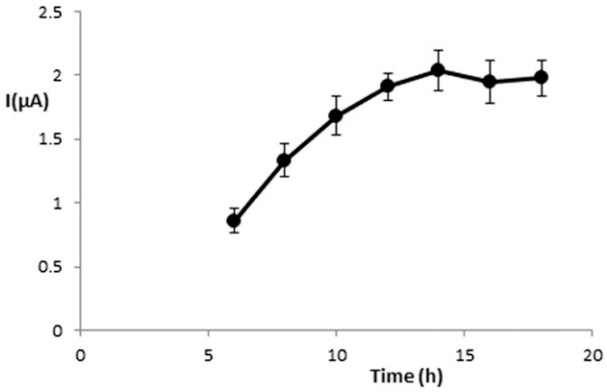

Figure 6. Effect of probe immobilization time on the peak current of DOX.

strands on the surface of the electrode. Au/GNP/Pr was thus immersed in 0.01 M Tris–HCl containing 0.9 mM HDM for 75 min. The resulting electrode, designated "Au/GNP/Pr-HDM," was first washed with ethanol and then TNE buffer.

Target Detection Using Au/GNP/Pr-HDM

Target detection using the biosensor as prepared included two steps: (*1*) hybridization between the immobilized probe and the target strands and (*2*) the stripping of voltammetry from DOX molecules that had intercalated into the duplexes that had formed. These steps are presented in Figure 2 and described in detail below.

*(**a**) Hybridization.*—For the detection of target strands, hybridization with immobilized probe strands should be performed first. Au/GNP/Pr-HDM was thus immersed in different concentrations of complementary or noncomplementary strands in SSC buffer at 50°C under constant stirring for 40 min. The electrode was then thoroughly rinsed with SSC buffer to remove any unhybridized strands.

*(**b**) Differential pulse-stripping voltammetry of DOX at the hybridized biosensor.*—To detect whether hybridization had occurred at the electrode surface, we used DOX, a well-known electroactive DNA intercalator. Hybridized Au/GNP/Pr-HDM was immersed in 10 μM DOX in 0.05 M phosphate buffer for 15 min under constant stirring. In this step, DOX molecules were intercalated, forming double-stranded DNA after hybridization and thus accumulating on the electrode surface. After washing the

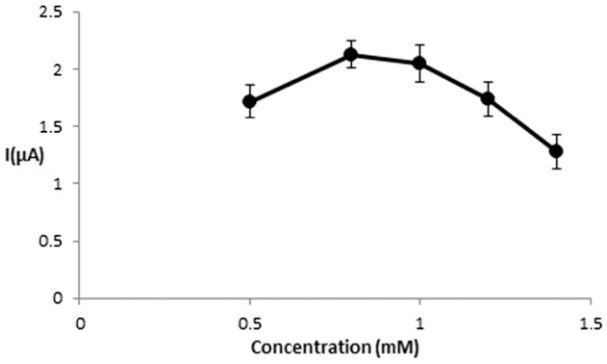

Figure 7. Effect of HDM concentration on the peak current of DOX.

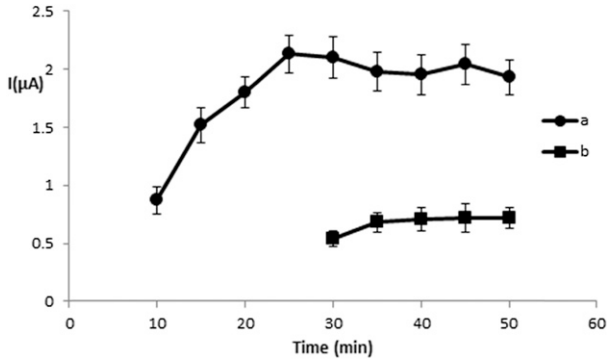

Figure 8. Effect of hybridization time on the peak current of DOX.

electrode, it was placed in phosphate buffer and the electrochemical signal of the accumulated DOX recorded.

Results and Discussion

Mechanism of Action for the Proposed Biosensor

When the prepared Au/GNP/Pr-HDM was immersed in the solution of the target strand, hybridization between the strands and strands that had immobilized on the electrode surface occurred. Consequently, the single-stranded probes became double-stranded. Incubation with DOX molecules resulted in the intercalation of these intercalators into duplexes and their subsequent draw to the electrode surface. Because DOX is an electroactive molecule, the electrochemical current of the intercalated DOX molecules correlated with their concentration and subsequently with the concentration of the target strands that formed duplexes.

Evaluation of the Preparation and Function of Au/GNP/Pr-HDM

To evaluate the efficiency of each step involved in the preparation of the biosensor and the biosensor's application for the measuring of the target concentration, at each step we investigated the cyclic voltammetry of the DOX molecules that had accumulated on the electrode surface. Figure 3 shows the cyclic voltammograms obtained at the surface of bare Au, Au/GNP, Au/GNP/Pr, Au/GNP/Pr-HDM, and hybridized Au/GNP/

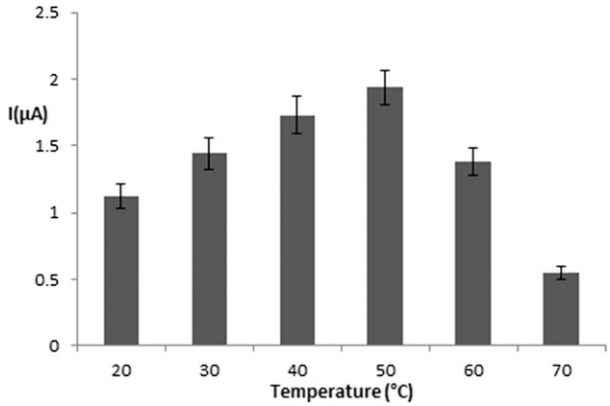

Figure 9. Effect of hybridization temperature on the peak current of DOX.

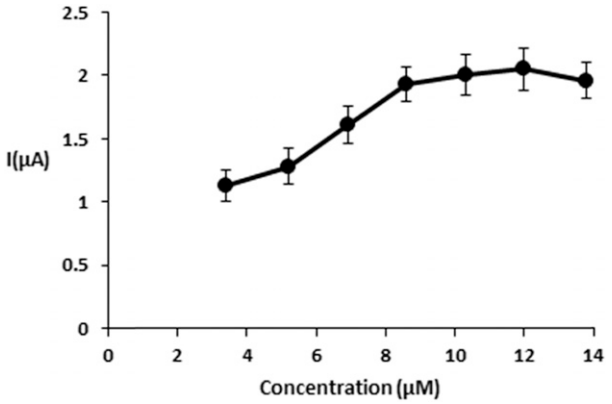

Figure 10. Effect of DOX concentration on the peak current of DOX.

Pr-HDM. At the surface of the bare Au electrode, a well-defined pair of oxidation and reduction peaks, respectively 577 and 605 mV, with a peak current ratio of 1, was observed, indicating a reversible electrochemical behavior for DOX. Modification of the electrode surface with GNP tripled peak currents. Immobilization of the thiolated probe strands increased peak currents by 1.8, suggesting interaction between the probes and DOX molecules. After immobilizing HDM, the reduction signal of DOX decreased 3-fold due to the blocking of the DOX molecules' direct route to the electrode surface. However, this decrease improved the sensitivity and LOD of the sensor. Preconcentration of DOX on the probe-modified surface was attributed to nonspecific hydrogen bonds. HDM displaced the nonspecifically adsorbed probes from the surface of the electrode. In addition, HDM resulted in good orientation of the probe strands, which stood vertically relative to the electrode surface, thus resulting in better hybridization with target strands (20). As can been seen in Figure 3, the electrochemical signal of DOX significantly increased after hybridization and subsequently formed double strands on the electrode surface, indicating DOX's higher tendency for double rather than single strands.

Refreshing the Biosensor Surface

To resuse Au/GNP/Pr-HDM, both DOX molecules and the hybridized target strands should be removed from the electrode surface. The hybridized electrode containing DOX was thus immersed into an 80°C water bath for 2 min. In this way, double strands were thermally denatured, thereby removing the target strands from the capture probes on the electrode surface. As shown in line b of Figure 4, after recovering the single-stranded probe, DOX's reduction signal decreased, but not sufficiently enough to touch the background line. Accordingly, DOX molecules were not removed; DOX molecules that had interacted with probe strands remained on the electrode surface. The electrode was immersed in 0.1 M phosphate-buffered saline under constant stirring for 5 min. High ionic strength resulted in the replacement of DOX molecules with sodium and potassium ions around the probe strands. As shown in line c of Figure 4, DOX's reduction signal completely disappeared. After hybridization of the target strands with the probes on the refreshed Au/GNP/Pr-HDM, the electrochemical current of the intercalated DOX showed no considerable difference compared with the initial electrochemical current (lines d and a in Figure 4). The obtained results showed that 20 consecutive uses of the biosensor, after refreshing its surface, reduced the electrochemical current to 97% of its initial value (data not shown).

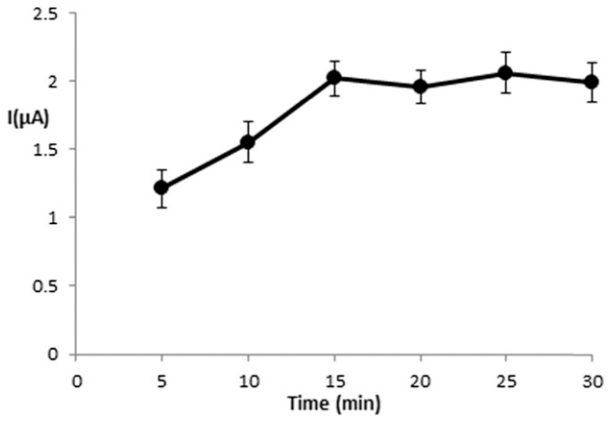

Figure 11. Effect of DOX accumulation time on the peak current of DOX.

Table 1. Specificity of the proposed biosensor

Strand	Amount added, nM	Peak current of DOX[a], μA
—[b]	—	0.34
Target	10.0	0.98
Noncomplementary A	10.0	0.36
Noncomplementary B	10.0	0.39

[a] Mean ± SD (n = 3).

[b] — = No miRNA strand.

Optimization of Experimental Parameters

To attain maximum sensitivity of the biosensor, different parameters influencing the sensor response were optimized.

Probe concentration.—Solutions containing different concentrations of the probe strands (0.5–1.5 μM) were used to modify the surface of Au/GNP. Figure 5 shows accumulated DOX reduction signals on the surface of each of the obtained sensors. As can be seen, increases in the concentration of the probe up to 1 μM increased the electrochemical signal. Further increases in concentration had no considerable effect on the signal. Thus, 1.2 μM was chosen as the optimal concentration.

Probe immobilization time.—The number of probe strands immobilized on an electrode surface undoubtedly influences detection sensitivity. In other words, the more probes immobilize, the higher the probability of hybridization; therefore, the higher the sensitivity. To immobilize the maximum number of probe strands, immobilization time was optimized. The obtained results show that 12 h was sufficient to efficiently immobilize the probes (Figure 6).

HDM concentration.—The effect of HDM concentrations in the range of 0.5–1.4 μM on the response of the sensor was investigated. According to the obtained results (Figure 7), the highest response was observed when 0.8–1 μM HDM was used to immobilize HDM. Lower concentrations were incapable of removing all nonspecifically adsorbed probes, and higher concentrations resulted in high accumulations of HDM on the surface, resulting in higher hydrophobicity, thereby decreasing

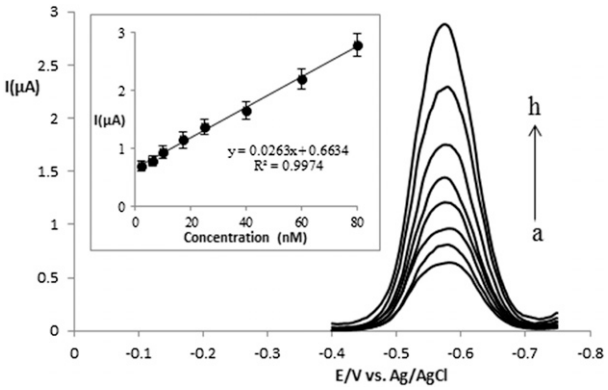

Figure 12. Stripped voltammograms from DOX at Au/GNP/Pr-HDM hybridized with different concentrations of the target strand. Lines a to h: 2, 6, 10, 17, 25, 40, 60, and 80 nM, respectively. The inset shows the calibration curve for the proposed biosensor extracted from the voltammograms.

the diffusion of hydrophilic DOX onto the electrode surface. Therefore, in subsequent experiments, 0.9 μM HDM was used for immobilization.

HDM immobilization time.—In addition to the surface coverage of the immobilized probe, the orientation of probe molecules attached to an electrode surface also affect hybridization, and subsequently, the electrochemical signal. Immobilizing HDM molecules between probe strands forces the probe strands to suitably orient themselves for hybridization with the target strands. Investigation of the effect of time on HDM immobilization revealed that 75 min was sufficient to block any remaining surface on the GNPs with HDM.

Hybridization time.—Hybridization time is an important factor that affects the complete hybridization of target and probe strands. To optimize hybridization time, the effects of different times (10–60 min) on the sensor response were evaluated. As shown in Figure 8, the reduction current of DOX increased as the hybridization time increased, and then leveled off. This experiment was carried out for two concentrations of the target: 50 and 5 nM. According to the obtained results, 50 nM required 25 min for maximum hybridization to occur, whereas 5 nM required 40 min. Therefore, 40 min was selected as the optimal hybridization time.

Hybridization temperature.—It has been demonstrated that the best hybridization of two complementary strands occurs at near-melting temperatures (28). The results obtained from investigating the effects of different temperatures on the hybridization, and subsequently, on the reduction current of accumulated DOX molecules, are reported in Figure 9. As can be seen, the most prominent signal was observed at 50°C.

DOX concentration.—The desired level of sensitivity and repeatability cannot be attained if an insufficient concentration of DOX is used, even if the sensor has been prepared and hybridized under optimal conditions. The effect of DOX concentrations in the range of 3.4–13.8 μM on the biosensor response was evaluated. As shown in Figure 10, increasing the concentration to 8.6 μM increased the electrochemical signal, whereas additional increases had no significant effect on the signal. Thus, 8.6 μM was selected as the optimal concentration of DOX.

Accumulation time.—Accumulation time here was defined as the interval of time DOX interacted with the double strands that had formed on the electrode surface. In this step, DOX molecules intercalated into hybridized strands and thus accumulated on the sensor surface where the electrochemical reduction would take place. Figure 11 shows the results of optimizing accumulation time. As can be seen, times greater than 15 min only increased analysis time without increasing electrochemical current. Thus, an accumulation time of 15 min was chosen for all subsequent experiments.

Specificity of the Proposed Biosensor

To evaluate the specificity of Au/GNP/Pr-HDM, its response to the complementary strand was compared with its two corresponding noncomplementary strands. Solutions containing 10 nM of the target strand, strand A and strand B, and a blank solution (SSC buffer) were separately analyzed using this approach. The results are listed in Table 1 and show that there was no considerable difference between the signals of the blank sample and strands A and B, whereas a well-defined signal was obtained for the target strand. Therefore, we concluded that the proposed biosensor was capable of specifically determining the target sequence.

Analytical Performance of the Proposed Method

The stripping of voltammograms from DOX that had accumulated on the surface of the hybridized Au/GNP/Pr-HDM at different concentrations of the target strand is illustrated in Figure 12. As shown, the dependence of DOX's peak height on the target concentration (Figure 12, inset) was linear in the range of 2–80 nM. The LOD, calculated as $3s_b$ (s_b = SD of seven blank measurements), was found to be 0.27 nM. To determine the reproducibility of the proposed assay, five similarly prepared Au/GNP/Pr-HDM sensors were used to analyze 15 nM of the target strand. The RSD value was ±6.7%.

Analytical Application

To test the applicability of the presented assay, different amounts of the target strand were added to aliquots of a human blood serum sample and then analyzed with the proposed approach using Au/GNP/Pr-HDM. The resulting data are reported in Table 2. The

Table 2. Results from the standard addition of the target strand to the serum sample

Sample	Amount added, nM	Amount found[a], nM	Recovery, %
Human blood serum	—[b]	—	—
	10.0	10.3 ± 0.7	103.0
	20.0	20.3 ± 1.3	101.5

[a] Mean ± SD (n = 3).

[b] — = Zero or no target strand.

obtained recovery values were 103 and 101.5%, indicating the reliability of the method for the determination of the complementary sequences in the serum samples.

Conclusions

We designed an electrochemical biosensor using DNA aptamers for probe and target strands to be used for the determination of miRNA-145 after RT-PCR. This approach was based on hybridization of the probe and target strands using DOX for the electrochemical transduction of hybridization. DOX, an electroactive intercalator, improved the sensitivity of the sensor because an extensive number of DOX molecules intercalated after each target strand was hybridized, thus accumulating on the surface of the electrode. We concluded that the proposed biosensor is simple, sensitive, specific, and rapid. Furthermore, if RT-PCR is performed before the electrochemical assay to convert each miRNA strand into a million DNA strands, additional amplification will occur; however, performance of the proposed biosensor coupled with RT-PCR will need to be investigated.

References

(1) Xu, Y., Cheng, G., He, P., & Fang, Y. (2009) *Electroanalysis* **21**, 1251–1259. doi:10.1002/elan.200804561

(2) Yuan, Q., Lu, D., Zhang, X., Chen, Z., & Tan, W. (2012) *Trends Analyt. Chem.* **39**, 72–86. doi:10.1016/j.trac.2012.05.010

(3) Gooding, J.J. (2002) *Electroanalysis* **14**, 1149–1156. doi:10.1002/1521-4109(200209)14:17<1149::AID-ELAN1149>3.0.CO;2-8

(4) Mohamadi, M., Mostafavi, A., & Torkzadeh-Mahani, M. (2014) *Biosens. Bioelectron.* **54**, 211–216. doi:10.1016/j.bios.2013.10.064

(5) Mohamadi, M., Mostafavi, A., & Torkzadeh-Mahani, M. (2015) *Bioelectrochemistry* **101**, 52–57. doi:10.1016/j.bioelechem.2014.07.003

(6) Mohamadi, M., Mostafavi, A., & Torkzadeh-Mahani, M. (2015) *J. Electrochem. Soc.* **162**, B344–B349. doi:10.1149/2.0581512jes

(7) Rezazadeh, F., Mohamadi, M., Afzali, D., Shamspur, T., & Mostafavi, A. (2015) *J. AOAC Int.* **98**, 1375–1381. doi:10.5740/jaoacint.15-042

(8) Drummond, T.G., Hill, M.G., & Barton, J.K. (2003) *Nat. Biotechnol.* **21**, 1192–1199. doi:10.1038/nbt873

(9) Yang, M., Li, Y., & Padgett, R.W. (2005) *Cytokine Growth Factor Rev.* **16**, 387–393. doi:10.1016/j.cytogfr.2005.02.008

(10) Riddihough, G. (2005) *Science* **309**, 1507. doi:10.1126/science.309.5740.1507

(11) Esquela-Kerscher, A., & Slack, F.J. (2006) *Nat. Rev. Cancer* **6**, 259–269. doi:10.1038/nrc1840

(12) Iorio, M.V., Ferracin, M., Liu, C.-G., Veronese, A., Spizzo, R., Sabbioni, S., Magri, E., Pedriali, M., Fabbri, M., & Campiglio, M. (2005) *Cancer Res.* **65**, 7065–7070. doi:10.1158/0008-5472.CAN-05-1783

(13) Michael, M.Z., O'Connor, S.M., van Holst Pellekaan, N.G., Young, G.P., & James, R.J. (2003) *Mol. Cancer Res.* **1**, 882–891

(14) Liu, X., Sempere, L.F., Galimberti, F., Freemantle, S.J., Black, C., Dragnev, K.H., Ma, Y., Fiering, S., Memoli, V., & Li, H. (2009) *Clin. Cancer Res.* **15**, 1177–1183. doi:10.1158/1078-0432.CCR-08-1355

(15) Gramantieri, L., Fornari, F., Ferracin, M., Veronese, A., Sabbioni, S., Calin, G.A., Grazi, G.L., Croce, C.M., Bolondi, L., & Negrini, M. (2009) *Clin. Cancer Res.* **15**, 5073–5081. doi:10.1158/1078-0432.CCR-09-0092

(16) Ichimi, T., Enokida, H., Okuno, Y., Kunimoto, R., Chiyomaru, T., Kawamoto, K., Kawahara, K., Toki, K., Kawakami, K., & Nishiyama, K. (2009) *Int. J. Cancer* **125**, 345–352. doi:10.1002/ijc.24390

(17) Amaral, F.C., Torres, N., Saggioro, F., Neder, L., Machado, H.R., Silva, W.A. Jr., Moreira, A.C., & Castro, M. (2009) *J. Clin. Endocrinol. Metab.* **94**, 320–323. doi:10.1210/jc.2008-1451

(18) Iorio, M.V., Visone, R., Di Leva, G., Donati, V., Petrocca, F., Casalini, P., Taccioli, C., Volinia, S., Liu, C.-G., & Alder, H. (2007) *Cancer Res.* **67**, 8699–8707. doi:10.1158/0008-5472.CAN-07-1936

(19) Schaefer, A., Jung, M., Mollenkopf, H.J., Wagner, I., Stephan, C., Jentzmik, F., Miller, K., Lein, M., Kristiansen, G., & Jung, K. (2010) *Int. J. Cancer* **126**, 1166–1176

(20) Zhou, Y., Wang, M., Meng, X., Yin, H., & Ai, S. (2012) *RSC Advances* **2**, 7140–7145. doi:10.1039/c2ra20487h

(21) Hamidi-Asl, E., Palchetti, I., Hasheminejad, E., & Mascini, M. (2013) *Talanta* **115**, 74–83. doi:10.1016/j.talanta.2013.03.061

(22) Zhang, G.-J., Chua, J.H., Chee, R.-E., Agarwal, A., & Wong, S.M. (2009) *Biosens. Bioelectron.* **24**, 2504–2508. doi:10.1016/j.bios.2008.12.035

(23) Pöhlmann, C., & Sprinzl, M. (2010) *Anal. Chem.* **82**, 4434–4440. doi:10.1021/ac100186p

(24) Cai, Z., Song, Y., Wu, Y., Zhu, Z., Yang, C.J., & Chen, X. (2013) *Biosens. Bioelectron.* **41**, 783–788. doi:10.1016/j.bios.2012.10.002

(25) Bartosik, M., Trefulka, M., Hrstka, R., Vojtesek, B., & Palecek, E. (2013) *Electrochem. Commun.* **33**, 55–58. doi:10.1016/j.elecom.2013.04.009

(26) Tymoczko, J.L., Berg, J.M., & Stryer, L. (2011) *Biochemistry: A Short Course*, Macmillan, London, England

(27) Wong, M.L., & Medrano, J.F. (2005) *Biotechniques* **39**, 75. doi:10.2144/05391RV01

(28) Dorak, M.T. (2007) *Real-Time PCR*, Taylor & Francis, New York, The United States